
ORIGINAL ARTICLE

Role of Magnetic Resonance Imaging in the Evaluation of Spinal Dysraphism

K Singh, CL Thukral, K Gupta, N Singh, SL Aggrawal, KS Ded

Department of Radiodiagnosis and Imaging, Sri Guru Ram Das Institute of Medical Sciences and Research, Amritsar, India

ABSTRACT

Objectives: This study aimed to characterise and categorise the site and type of spinal dysraphism as seen on magnetic resonance imaging (MRI), to study additional / associated findings in cases of spinal dysraphism, and correlate the MRI findings with surgical and / or anatomical and pathological findings wherever possible.

Methods: We prospectively studied 50 patients who presented with a clinical diagnosis of spinal dysraphism and referred to the Department of Radiodiagnosis and Imaging, Sri Guru Ram Das Institute of Medical Sciences and Research in India for MRI from January 2014 to June 2015. All patients underwent a detailed physical examination, followed by MRI.

Results: Most patients (74%) were younger than 1 year. The incidence of spinal dysraphism was higher in males (male-to-female = 1.08:1). Of the 50 patients, open spinal dysraphism was observed in 24 and closed spinal dysraphism in 26. The lumbar region was the most common site of occurrence (54.2%), followed by the sacral region (33.3%). There was an excellent agreement (kappa value = 0.937) for the evaluation of spinal dysraphism between MRI and histopathological assessments. A final histopathological diagnosis was obtained in 34 patients.

Conclusion: MRI of the spine is a safe, non-invasive, and quick method of describing the multiple findings in patients with spinal dysraphism and also serves as a highly accurate diagnostic mode of imaging.

Key Words: Magnetic resonance imaging; Meningocele; Neural tube defects; Spinal dysraphism

中文摘要

MRI在評估脊神經管閉合不全的作用

K Singh, CL Thukral, K Gupta, N Singh, SL Aggrawal, KS Ded

目的：本研究利用MRI找出脊神經管閉合不全的位置和種類，並把它們分類。此外，亦研究了有關脊神經管閉合不全的更多相關表現，並盡可能找出MRI診斷與手術 / 解剖結果的相關性。

方法：本研究報導在2014年1月至2015年6月期間印度Sri Guru Ram Das醫學研究所為曾因脊神經管閉合不全而轉介至我們機構的50名病人作前瞻性研究。所有病人均須接受詳細的身體檢查，隨後進行MRI。

結果：大多數患者（74%）年齡小於1歲。男性脊神經管閉合不全的發病率高於女性（男女比例為

Correspondence: Dr Kunwarpal Singh, 1806/7-12, Bazar Ghumiaran, Chowk Lachhmanisar, Opposite darshan maternity home, Amritsar 143006 (Punjab), India
Email: kpsdhami@hotmail.com

Submitted: 29 Sep 2015; Accepted: 21 Mar 2016.

Disclosure of Conflicts of Interest: All authors have disclosed no conflicts of interest.

1.08 : 1) 。50例中有24例屬開放式，另26例屬封閉式。腰部為最常見的部位 (54.2%)，其次為骶區 (33.3%)。MRI診斷結果與病理組織學診斷高度一致 (kappa值=0.937)。34名病人最終由病理組織學確診。

結論： 脊柱MRI能為脊神經管閉合不全的病人提供一個安全、非侵入性和快捷的方法作多處病情描述，同時亦能提供高度精確的成像診斷模式。

INTRODUCTION

The term dysraphism refers to defective closure of the neural tube and therefore should apply to abnormalities of primary neurulation only. Nonetheless its application has been broadened to include all congenital spinal disorders in which there is anomalous differentiation and / or incomplete closure of dorsal midline structures including skin, muscles, vertebrae, meninges, and nervous tissue.¹

The true incidence of spinal dysraphism in the general population is unknown,¹ although an incidence of 0.05 to 0.25 per 1000 births has been estimated.² These abnormalities usually involve the lumbosacral spine, although lesions in the cervical and thoracic regions do occur.²

From a clinical and embryological perspective, the disorders of primary neurulation can be divided into open spinal dysraphism (OSD) and closed spinal dysraphism (CSD). In OSD, neural tissue is exposed to the skin with leakage of cerebrospinal fluid (CSF). In CSD, the malformed neural tube is covered by mesodermal (subcutaneous fat) and ectodermal (skin) elements; no neural tissue is freely exposed and no leakage of CSF is present.³

Magnetic resonance imaging (MRI) became the most useful modality for detailed imaging of the anatomy of these lesions and was reported as the imaging study of choice for spinal dysraphism in 1986.⁴

The present study aimed to characterise and categorise the site and type of spinal dysraphism on MRI, study additional / associated findings in cases of spinal dysraphism, and correlate the MRI findings with surgical and / or anatomical pathological findings wherever possible.

METHODS

We prospectively studied 50 patients of all age-groups with a clinical diagnosis of spinal dysraphism over a

period of 18 months from January 2014 to June 2015. The study was approved by the hospital research and ethics committee. Informed consent was obtained from all study participants. Patients were excluded from the study if they had had previous surgery for spinal dysraphism and / or there were contraindications to MRI. All patients included in the study were subjected to a physical examination and a detailed clinical history was obtained.

MR Technique and Protocol

MRI in the present study was carried out on a Philips Gyroscan Achieva 1.5 Tesla unit (Philips, Amsterdam, The Netherlands). The standard protocol consisted of T1-weighted (T1W) sequence in axial and sagittal planes, T2-weighted (T2W) sequence in axial, sagittal, and coronal planes. Short tau inversion recovery sequence was used wherever required. For brain screening, T2W sequence in sagittal and axial planes were used.

RESULTS

During January 2014 to June 2015, patients of all age-groups who presented to the Department of Surgery with a clinical diagnosis of spinal dysraphism and who subsequently underwent MRI in the Department of Radiodiagnosis & Imaging at Sri Guru Ram Das Institute of Medical Sciences and Research in India were recruited. All patients had undergone thorough clinical examination.

A total of 50 patients (26 male and 24 female) were examined using MRI. The mean age was 2.8 years, with a range from 1 day to 15 years. Most patients (74%) were younger than 1 year, 14% were 1 to 5 years old, and 12% older than 5 years. Clinically all patients presented with either a skin-covered or non-skin-covered back mass. Of the 50 patients, 26 had CSD and 24 had OSD. Various features were present in CSD patients, but all the OSD patients presented with meningocele (MMC). Their features are listed in Table 1. Of the 12 patients with diastematomyelia, eight were associated with CSD abnormalities and four with

Table 1. Type and frequency of dysraphic lesions and associated congenital spinal anomalies in studied patients.

Type	Features (No. of patients)	Associated congenital spinal lesions (No. of patients)
Open spinal dysraphism	Meningomyelocele (24)	Syringohydromyelia (13)
		Tethered cord (19)
Closed spinal dysraphism	Lipomyelomeningocele (4)	Kyphoscoliosis (5)
		Hemivertebrae (4)
		Block vertebrae (2)
		Diastematomyelia (4)
		Partial sacral agenesis (1)
		Ventriculomegaly (9)
	Meningocele (3)	Corpus callosum agenesis (5)
		Arnold-Chiari type II (5)
		Syringohydromyelia (1)
		Tethered cord (4)
		Block vertebrae (1)
		Kyphoscoliosis (2)
	Diastematomyelia (8)	Tethered cord (2)
		Diastematomyelia (1)
		Hemivertebrae (2)
		Epidural lipoma (1)
		Syringohydromyelia (8)
		Tethered cord (7)
Filum terminale lipoma (2) Dorsal dermal sinus (11)	Dorsal dermal sinus (1)	
	Kyphoscoliosis (3)	
	Block vertebra (3)	
	Hemivertebra (3)	
	Partial sacral agenesis (1)	
	Epidural lipoma (2)	
	Ventriculomegaly (4)	
	Corpus callosum agenesis (1)	
	Arnold-Chiari type II (2)	
	Arnold-Chiari type III (2)	
Tethered cord (2)		
Meningomyelocele (cervical) (2)	Syringohydromyelia (6)	
	Tethered cord (3)	
	Kyphoscoliosis (3)	
	Block vertebra (3)	
	Hemivertebra (1)	
	Diastematomyelia (1)	
	Partial sacral agenesis (1)	
	Epidural arachnoid cyst (1)	
	Ventriculomegaly (1)	
	Corpus callosum agenesis (1)	
Arnold-Chiari type III (2)		
	Corpus callosum agenesis (1)	
	Ventriculomegaly (1)	
	Arnold-Chiari type II (1)	

OSD. Epidural arachnoid cyst was seen in association with CSD in one patient.

The lumbar region (54.2%) was the most common site of occurrence of spinal dysraphism, followed by the sacral (33.3%), thoracic (8.3%), and cervical (4.2%) regions (Table 2).

Chiari II malformation was diagnosed in eight patients as an associated finding in dysraphic lesions (all patients had MMC and 3 patients had diastematomyelia).

Table 2. Distribution of patients with congenital spinal lesions on the basis of level of spine involvement.

Level	No. (%) of patients
Cervical	2 (4.2)
Thoracic	4 (8.3)
Lumbar	26 (54.2)
Sacral	16 (33.3)

Chiari III malformation was present in four patients, of whom two had associated dorsal dermal sinus and two had diastematomyelia.

Syringohydromyelia was detected as an associated finding in 13 OSD and 16 CSD dysraphic patients. The final diagnosis was made by surgery / histopathology in 34 patients with an excellent correlation ($\kappa = 0.937$) between MRI and histopathology assessments. MRI was erroneous in giving a provisional diagnosis of meningocele in one case that on subsequent surgery and histopathology it was found to be MMC. On retrospective review, this case presented with a swelling in the lumbosacral spine. MRI spine and brain was performed and reported by a resident in a peripheral hospital, who had mistaken the neural tissue within the MMC as meninges only. Surgery was not performed in six patients due to anticipated neurological complications and a further 10 patients refused surgery. Examples of some cases are shown in Figures 1 to 4.

DISCUSSION

In the present study, the majority of cases were male ($n = 26$; 52%) with a male-to-female ratio of 1.08:1. Nishtar et al⁵ reported a similar male-to-female ratio of 1.12:1.

The majority of patients were found to have MMC and constituted about 52% of the study population with most lesions (87.5%) located in the lumbosacral region. This is in agreement with Kumar and Singh⁶ who stated that MMC is the most common skin manifestation and the lumbosacral region the most common site of spinal dysraphism. MR examination showed defective posterior elements in all cases with meningeal sac filled with CSF and neural tissue. This is in agreement with Tortori-Donati et al⁷ who stated that in MMC,

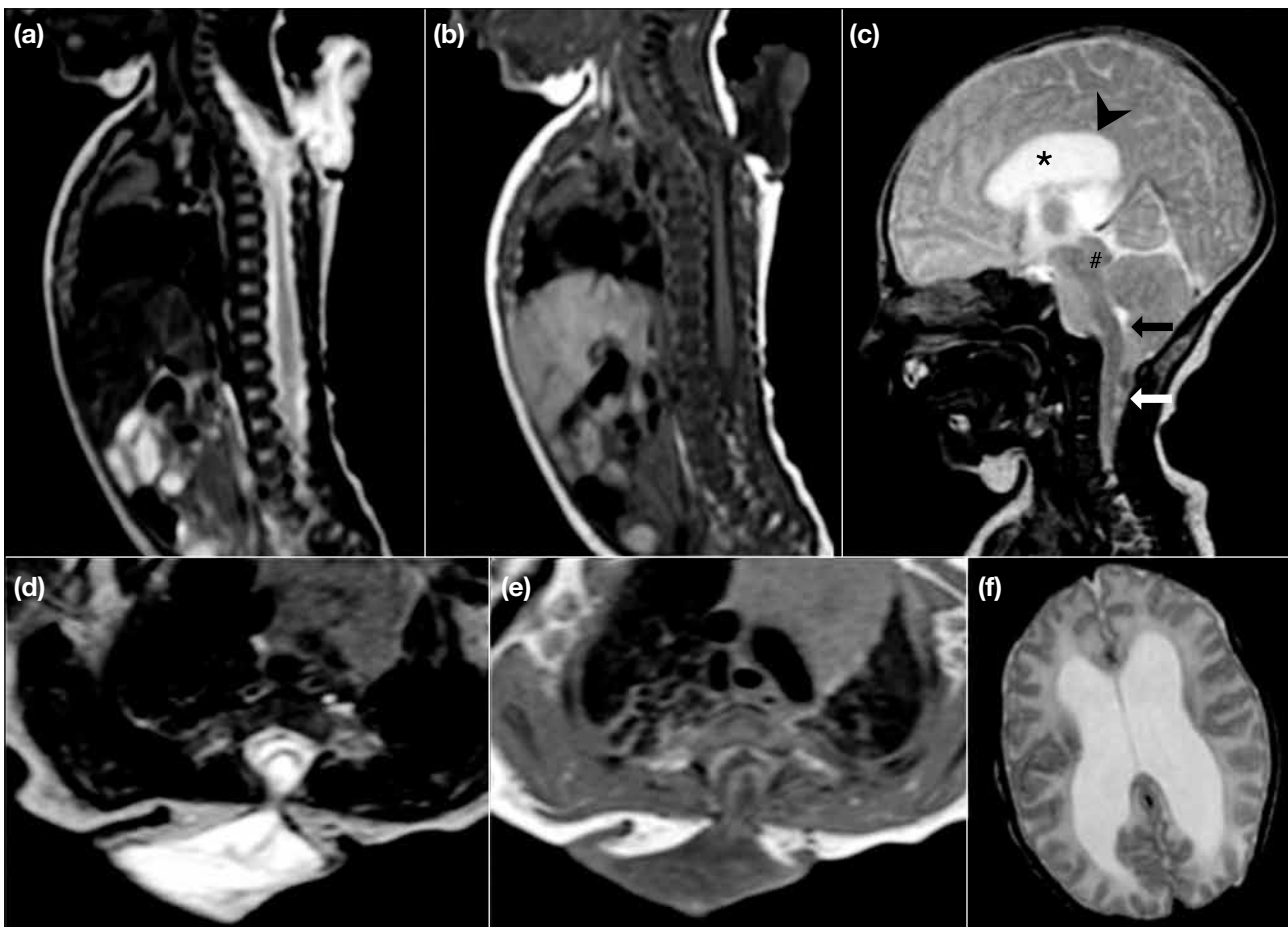


Figure 1. Myelomeningocele with tonsillar herniation (Arnold-Chiari malformation type II). T2-weighted (a) sagittal and (d) axial, and T1-weighted (b) sagittal and (e) axial images show a spina bifida defect in the upper thoracic region through which cerebrospinal fluid, cord, meninges, and nerve roots are herniating into a sac-like structure. (c) T2-weighted sagittal image shows herniation of tonsils (white arrow), dilatation of lateral ventricles (*), thinning of corpus callosum (arrowhead), beaked tectum (#), and small compressed 4th ventricle (black arrow). (f) T2-weighted axial brain image shows dilatation of lateral ventricles.

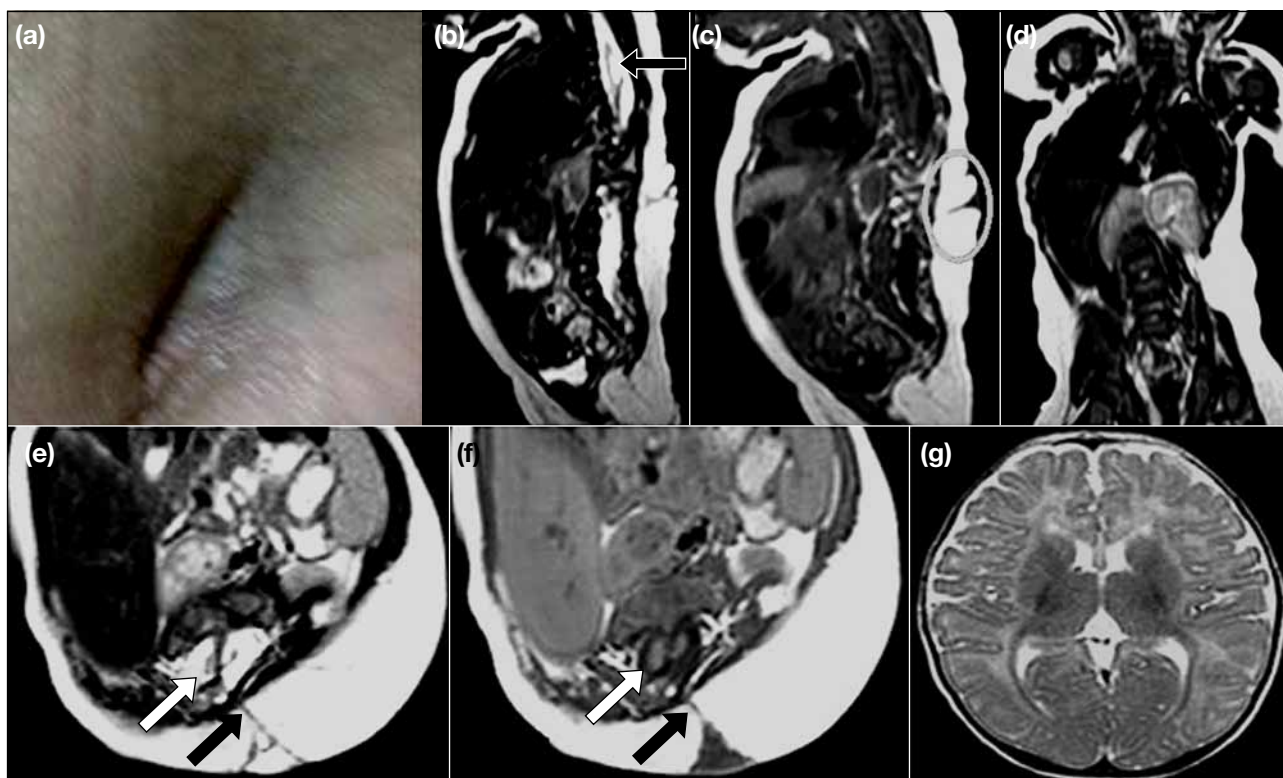


Figure 2. Dorsal dermal sinus with diastematomyelia. (a) A sinus tract extending deep from the skin surface. (b) T2-weighted sagittal image shows syringohydromyelia (arrow) in the dorsal region. (c) T1-weighted sagittal image shows a dorsal dermal sinus tract extending from the skin surface (circle). (d) T2-weighted coronal image shows scoliotic deformity of the spine towards the left side. (e) T2- and (f) T1-weighted images show dorsal dermal sinus tract (black arrows) extending from the skin surface up to the lamina although no intradural extension is noted and bony septum splitting the spinal cord (white arrows) into two hemicords seen in two dural sacs (diastematomyelia type I). (g) T2-weighted axial image shows normal brain parenchyma and ventricles.

a segment of the spinal canal (placode) protrudes together with the meninges through a bony defect in the midline of the back, and is therefore exposed to the environment.

The spinal cord showed syringohydromyelia in 13 patients. This is in agreement with Kumar and Singh⁶ who stated that syringohydromyelia was the common association in MMC. In this study, sagittal MRI sections in the craniocervical region showed tonsillar herniation i.e. Chiari type II malformation in eight patients.

Meningocele was initially diagnosed in three patients by MRI but one case was subsequently found to be MMC after surgery and histopathology. Meningocele thus constituted 4% of all cases of spinal dysraphism. For the two patients who were correctly diagnosed by MRI with MMC, one had associated hypertrichosis, diastematomyelia, and low-lying tethered cord. The findings of the present study are consistent with the

work by Kumar and Singh⁶ in which three out of 155 patients presented with meningocele. The classical posterior meningocele is characterised by herniation of a CSF-filled sac lined by dura mater and arachnoid through posterior spina bifida. It is commonly lumbar or sacral, but thoracic and even cervical meningoceles are occasionally found.⁸

Lipomyelomeningocele was detected in four patients in our study, all of whom presented with a skin-covered midline back mass just above the intergluteal crease. The mass was soft in consistency with areas of nevi on the back in one patient. This is in agreement with Tortori-Donati et al⁸ who stated that a midline subcutaneous mass right above the natal cleft and extending asymmetrically into one buttock is the rule. On MR examination the subcutaneous and intramedullary lipoma showed hyperintense signal on both T1W and T2W sequences. The spinal cord was low lying and tethered by the lipomatous tissue in all

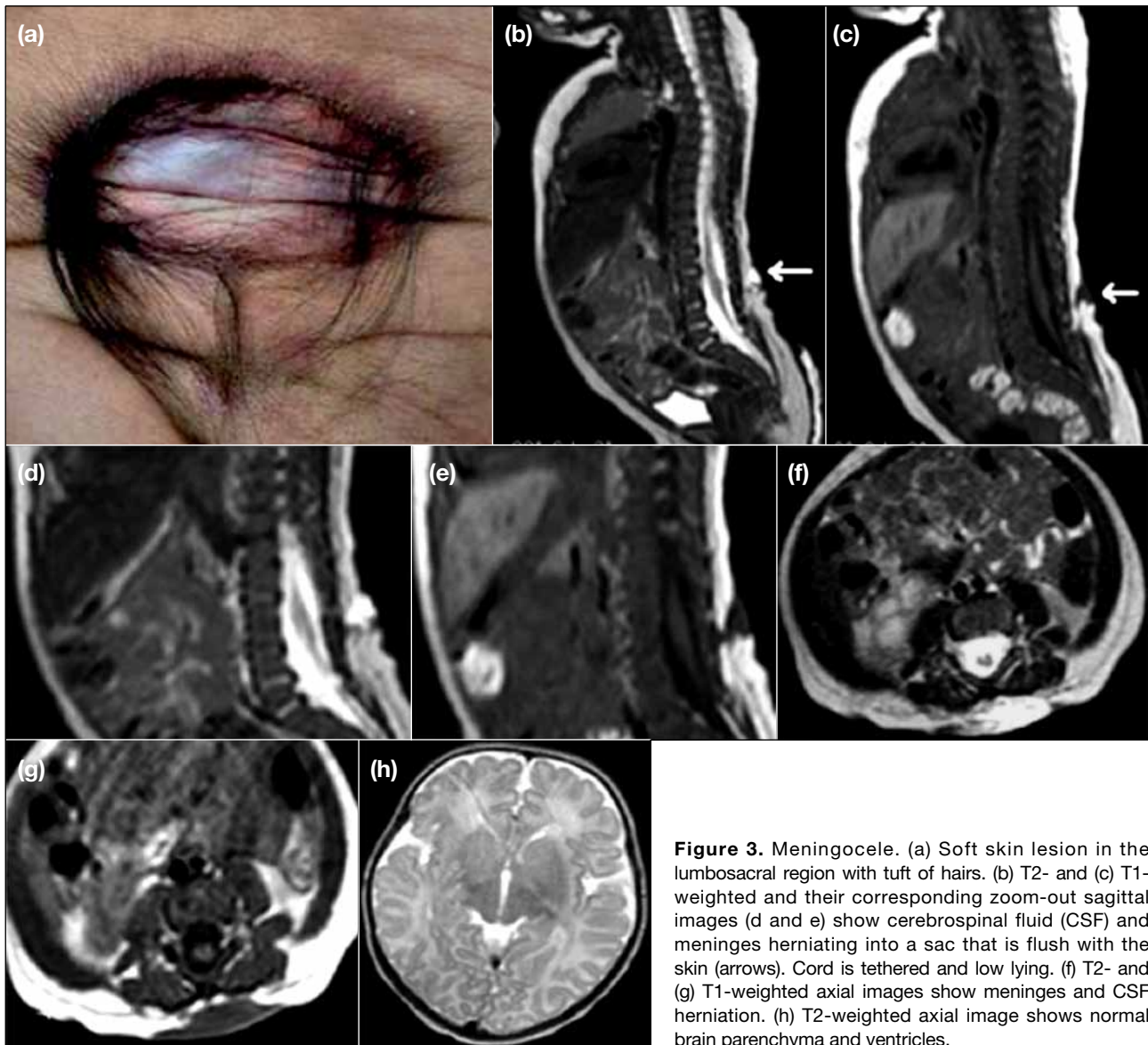


Figure 3. Meningocele. (a) Soft skin lesion in the lumbosacral region with tuft of hairs. (b) T2- and (c) T1-weighted and their corresponding zoom-out sagittal images (d and e) show cerebrospinal fluid (CSF) and meninges herniating into a sac that is flush with the skin (arrows). Cord is tethered and low lying. (f) T2- and (g) T1-weighted axial images show meninges and CSF herniation. (h) T2-weighted axial image shows normal brain parenchyma and ventricles.

the patients. This is in agreement with DeLaPaz et al⁹ who stated that the spinal cord is almost always in a low position with conus in the lower lumbar or sacral canal.

Kilickesmez et al¹⁰ and Moorthy¹¹ reported that diastematomyelia referred to an abnormality where the spinal canal was split by a fibrous, cartilaginous, or bony septum creating two sleeves, each containing a portion of spinal cord that was split sagittally. The incidence of diastematomyelia in our study was 24% while the incidence was 20% to 40% in the study by McComb.¹² On MR examination, spur may be isointense or slightly hyperintense compared with CSF on T1W images if non-ossified; it will be hyperintense on T1W images if

ossified because of the high signal intensity of marrow. Bony, cartilaginous, and fibrous spurs all appeared hypointense on T2W spin echo and gradient echo images. This is in agreement with Kilickesmez et al's study.¹⁰

Tortori-Donati et al⁷ stated that the dermal sinus was an epithelium-lined fistula that extends inward from the skin surface, and could connect with the central nervous system and the meningeal coating. Dermal sinus tract was found in 22% of patients in our study, similar to a study by Nishtar et al⁵ which showed an incidence of 17.6%. MR examination showed the sinus tract as a hypointense tract on T1W sequence connecting the skin

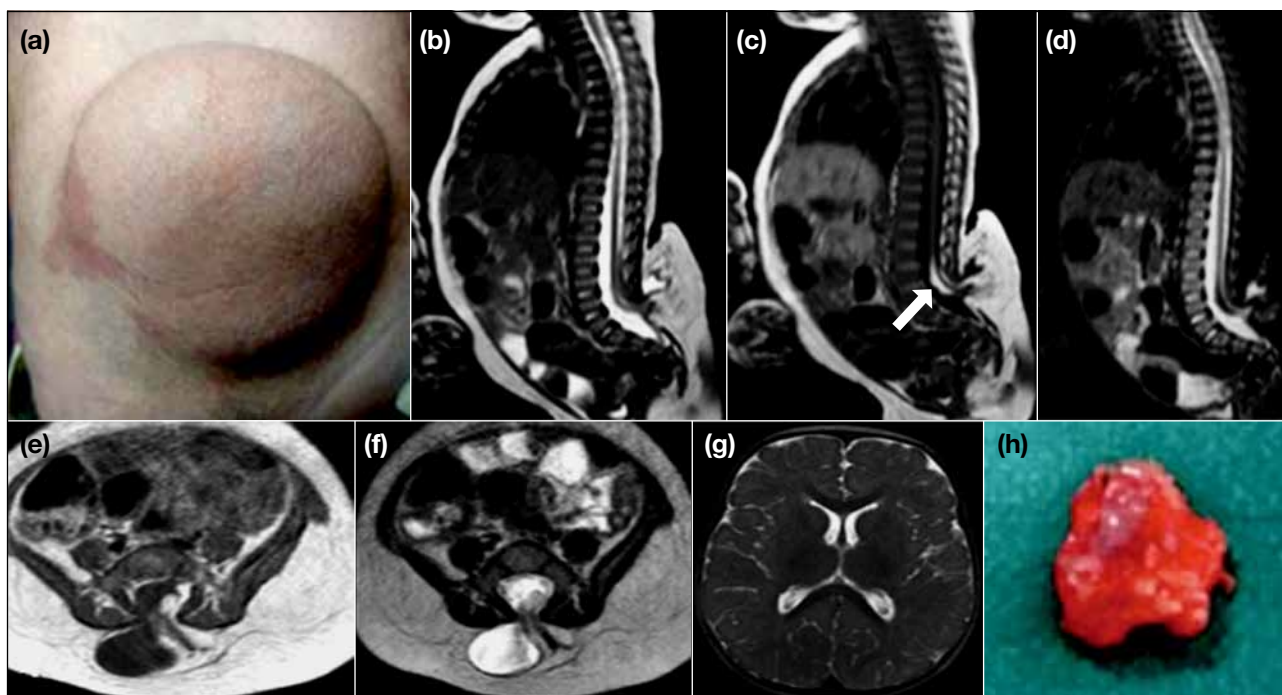


Figure 4. Lipomyelomeningocele with filum terminale lipoma. (a) Subcutaneous swelling in the lumbosacral region with skin pigmentation. T2-weighted (b) sagittal and (f) axial, and T1-weighted (c) sagittal and (e) axial images show a spina bifida defect in the lumbosacral region through which cerebrospinal fluid, cord, meninges, fat, and nerve roots are herniating into a sac-like structure. Cord is tethered and low lying. Placode lipoma interface lies outside the anatomical boundaries of spinal canal. (c) Fat signal intensity lesion is seen in the region of filum terminale on T1-weighted images: filum terminale lipoma (arrow). (d) Corresponding short T1 inversion recovery sagittal image shows loss of fat signal (appears hypointense). (g) T2-weighted axial image shows normal brain parenchyma and ventricles. (h) Postoperative tissue specimen: an irregular haemorrhagic soft tissue piece measuring 3 x 2 x 1.5 cm in size. External surface shows irregular areas of congestion. On cut surface, few areas of grey white fibrofatty tissues are seen.

to the subarachnoid space. This is similar to the findings described by Jindal and Mahapatra¹³ who stated that all midline skin dimples above the intergluteal crease must be assumed to communicate intraspinally and those below the crease are blind sacrococcygeal dimples and do not require exploration.

Filum terminale lipoma is commonly seen at the lumbosacral level and accounted for 4% of spinal dysraphism in our study compared with 3.2% in a study by Al-Omari et al.¹⁴ On MRI, filum lipomas are isointense to subcutaneous fat in all sequences i.e. they give high signal on T1W and fast spin echo T2W images. Filum terminale lipoma on MRI shows fat within thickened filum terminale. Because the filum terminale is slightly off the midline, axial T1W images are most useful for diagnosis. This is in agreement with study done by Tortori-Donati et al.⁸

Spinal dysraphic lesions can anatomically tether the conus medullaris so that the neural tissue of the lower

spinal cord is placed in progressive mechanical traction as the child's vertebral column grows. It is therefore postulated that over time, progressive cord ischaemia and neural dysfunction will result.⁵ In our study, tethered cord was seen in 58% of patients compared with the 64.7% reported by Nishtar et al.⁵

We included eight patients with Chiari II malformation in our study, including five females and three males. A similar incidence was found by Hadley,¹⁵ where Chiari II malformation affected girls twice as often as boys. All patients had MMC and there was associated diastematomyelia in three. MRI examination revealed caudal herniation of the cerebellar tonsil, as well as herniation of the brain stem, 4th ventricle and shallow posterior fossa. Hydrocephalus (6 patients) and syringohydromyelia (6 patients) were associated features that have been reported by Griffiths et al,¹⁶ of whom four presented with Chiari II malformation, two had associated dorsal dermal sinus, and two had diastematomyelia.

Our study showed excellent agreement ($\kappa = 0.937$) for the evaluation of spinal dysraphism between MRI and histopathological assessment. Preoperatively, the final diagnosis was accurately made on the basis of MRI in 33 out of 34 patients. These results are similar to those of Altman and Altman¹⁷ who evaluated and correlated the diagnostic performance of MRI with surgery / histopathological sections and observed a high correlation between the values measured by MRI and histopathology. In our study, MRI showed high accuracy of 97.4% in evaluation of spinal dysraphism and supports the findings of Nishtar et al⁵ who stated that MRI is a highly accurate modality in the diagnosis of spinal dysraphism.

CONCLUSION

MRI is an excellent means to image pathological processes in the paediatric spine. Because of its multiplanar imaging and tissue characterisation abilities, MRI plays a key role in the diagnosis of spinal dysraphism. MRI is useful in detecting spinal dysraphism that may be missed by conventional radiological evaluation, physical examination, and spinal ultrasound. MRI is also an excellent modality for identification of neural tissue abnormalities associated with spinal dysraphism such as syringohydromyelia, spinal lipomas, tethered cord, hydrocephalus, vertebral anomalies, and Chiari malformations.

REFERENCES

- Naidich TP, Zimmerman RA, McLone DG. Congenital anomalies of the spine and spinal cord. In: Atlas SW, editor. Magnetic resonance imaging of the brain and spine. 2nd ed. Philadelphia: Lippincott-Raven; 1996. p 1265-337.
- Warder DE. Tethered cord syndrome and occult spinal dysraphism. *Neurosurg Focus*. 2001;10:e1. [crossref](#)
- Huisman TA, Rossi A, Tortori-Donati P. MR imaging of neonatal spinal dysraphia: what to consider? *Magn Reson Imaging Clin N Am*. 2012;20:45-61. [crossref](#)
- Warf BC. Pathophysiology of tethered cord syndrome. In: McLone DG, editor. Pediatric neurosurgery: surgery of the developing nervous system. 4th ed. Philadelphia: WB Saunders; 2001. p 182-5.
- Nishtar T, Elahi A, Iqbal N. To determine the frequency of accuracy of MRI in diagnosis of rare disorder of spinal dysraphism. *J Med Sci*. 2011;19:195-9.
- Kumar R, Singh SN. Spinal dysraphism: trends in northern India. *Pediatr Neurosurg*. 2003;38:133-45. [crossref](#)
- Tortori-Donati P, Rossi A, Biancheri R, Cama A. Magnetic resonance imaging of spinal dysraphism. *Top Magn Reson Imaging*. 2001;12:375-409. [crossref](#)
- Tortori-Donati P, Rossi A, Cama A. Spinal dysraphism: a review of neuroradiological features with embryological correlations and proposal for a new classification. *Neuroradiology*. 2000;42:471-91. [crossref](#)
- DeLaPaz RL, Enzmann DR, Rubin JB. Congenital anomalies of the spine and spinal cord. In: Enzmann DR, DeLaPaz RL, Rubin JB, editors. Magnetic resonance of the spine. St. Louis: Mosby; 1990.
- Kilickesmez O, Tafldemiroglu E, Inci E, Bayramoglu S, Cimilli T. Split spinal cord malformations and associated spinal anomalies: comparison of MRI findings with intraoperative results. *Med J Bakirkoy*. 2007;3:142-6.
- Moorthy S. Split notochord syndrome. *Neurol India*. 2003;49:128-31.
- McComb JG. Spinal and cranial neural tube defects. *Semin Pediatr Neurol*. 1997;4:156-66. [crossref](#)
- Jindal A, Mahapatra AK. Spinal congenital dermal sinus: an experience of 23 cases over 7 years. *Neurol India*. 2001;49:243-6.
- Al-Omari MH, Eloqayli HM, Qudseih HM, Al-Shinag MK. Isolated lipoma of filum terminale in adults: MRI findings and clinical correlation. *J Med Imaging Radiat Oncol*. 2011;55:286-90. [crossref](#)
- Hadley DM. The Chiari malformations. *J Neurol Neurosurg Psychiatry*. 2002;72 Suppl 2:ii38-ii40.
- Griffiths PD, Wilkinson ID, Variend S, Jones A, Paley MN, Whitby E. Differential growth rates of the cerebellum and posterior fossa assessed by post mortem magnetic resonance imaging of the fetus: implications for the pathogenesis of the chiari 2 deformity. *Acta Radiol*. 2004;45:236-42. [crossref](#)
- Altman NR, Altman DH. MR imaging of spinal dysraphism. *AJNR Am J Neuroradiol*. 1987;8:533-8.